Distributed Optimization in Energy Harvesting Sensor Networks with Dynamic In-network Data Processing

Shusen Yang
University of Liverpool
Email: shusen.yang@liverpool.ac.uk

Yad Tahir
Imperial College London
Email: y.tahir11@imperial.ac.uk

Po-yu Chen
Imperial College London
Email: po-yu.chen11@imperial.ac.uk

Alan Marshall
University of Liverpool
Email: Alan.Marshall@liverpool.ac.uk

Julie McCann
Imperial College London
Email: j.mccann@imperial.ac.uk

***Abstract*—Energy Harvesting Wireless Sensor Networks (EH-WSNs) have been attracting increasing interest in recent years. Most current EH-WSN approaches focus on sensing and networking algorithm design, and therefore only consider the energy consumed by sensors and wireless transceivers for sensing and data transmissions respectively. In this paper, we incorporate CPU-intensive edge operations that constitute in-network data processing (e.g. data aggregation/fusion/compression) with sensing and networking; to jointly optimize their performance, while ensuring sustainable network operation (i.e. no sensor node runs out of energy). Based on realistic energy and network models, we formulate a stochastic optimization problem, and propose a lightweight on-line algorithm, namely Recycling Wasted Energy (RWE), to solve it. Through rigorous theoretical analysis, we prove that RWE achieves asymptotical optimality, bounded data queue size, and sustainable network operation. We implement RWE on a popular IoT operating system, Contiki OS, and evaluate its performance using both real-world experiments based on the FIT IoT-LAB testbed, and extensive trace-driven simulations using Cooja. The evaluation results verify our theoretical analysis, and demonstrate that RWE can recycle more than 90% wasted energy caused by battery overflow, and achieve around 300% network utility gain in practical EH-WSNs.**

I. Introduction

Modern energy harvesting technologies have enabled wireless sensor networks (WSNs) and the emerging Internet of Things (IoTs) to operate in a more autonomous fashion; powered by renewable energy sources such as solar [1], vibration [2], and wireless energy transfer [3]. Sustainable operation promotes the ubiquitous deployment of energy harvesting sensing systems (EH-WSNs), making IoT a major source of big data. However, due to the limited energy harvesting capacities of typically tiny devices, energy remains a scarce resource. Furthermore, renewable energy is inherently time-varying and exhibits a high degree of heterogeneity over different sensor nodes. This has opened a new dimension for sensing and networking algorithm design, which has been attracting an growing research interest in recent years [4], [5].

In addition to efficient energy utilization, network congestion is an issue that becomes heightened due to exponentially increasing volumes of IoT data being transmitted over the limited wireless spectrum resource [6]. An efficient way to reduce bandwidth consumption is via *in-network data processing*, where data is processed and reduced inside the network. Typical in-network processing operations for IoT data collections include raw sensor data compression, aggregation, fusion, and feature extraction [7]–[9]. Beside data volume reduction, in-network processing can also be viewed as data pre-processing during the data acquisition phase, which can significantly improve the efficiency and quality of overall IoT data analytics (e.g. computational overhead reduction caused by dimensionality reduction [10] and accuracy improvement due to data cleaning [11]).

Since both energy harvesting and in-network data processing are important IoT techniques, it is essential to study them jointly. Because data processing operations are normally CPU-incentive and therefore consume energy, the key research issue here is to jointly optimize sensing (rate control), networking (routing, scheduling, and data forwarding), and in-network data processing for highly dynamic EH-WSNs. To our knowledge, this triplet optimization has not been studied yet.

A. Contributions

This paper presents both theoretical and practical studies on how to optimize network performance in EH-WSNs through in-network data processing while also ensuring sustainable network operation (i.e. no device runs out of energy). Our contributions are summarized as follows:

1. For system modeling, we propose a novel approach called *shadow sink* to map data processing to virtual data forwarding operations, in order to seamlessly combine data processing and wireless networking. We also establish realistic models for energy harvesting, energy storage (i.e. rechargeable battery with finite capacity), and four energy consumption

operations: sensing, data transmitting, data receiving, and in-network data processing. Based on these models, a stochastic optimization problem is formulated to maximize the aggregate network utility while guaranteeing sustainable network operation for EH-WSNs with arbitrary network topologies and dynamics.

2. To solve the formulated problem in real-time, we develop an adaptive algorithm, Recycling Wasted Energy (RWE), that uses the Lyapunov optimization technique [12]. We present two versions of RWE: an optimal partially-distributed approach (RWE-opt) and a sub-optimal fully-distributed approach (RWE-dist). To our knowledge, RWE is not only the first in-network data processing approach that considers both energy and networking limitations in EH-WSNs, but also the first approach that applies in-network data fusion to the Lynaponov optimization framework.

3. Through rigorous theoretical analysis, we prove three highly desired properties of RWE: bounded data queue sizes (for limited storage resource of typical sensor nodes), sustainable operation, and asymptotical optimality.

4. We implement RWE-dist in the open source IoT operating system Contiki [13]. Through both experiments on the FIT IoT-LAB testbed [14] and extensive trace-driven simulations on Cooja (i.e. simulator for Contiki [13]), we demonstrate that RWE manages to improve network performance significantly in practical EN-WSNs, in terms of harvested energy utilization, network utility, and network throughput.

B. Related Work

1) Energy Harvesting Networks: There exist a large body of theoretical and practical research results in EH-WSNs [15], including power management schemes [1], [16], [17], routing [1], sensing [1], [18], [19], and path traveling optimization in WSNs using wireless power transfer [20]. Recent approaches that use Lyapunov optimization techniques [12] for joint power management and network optimization [4], [5], [21], are most relevant to our work. However, none of these work consider in-network processing or complete energy consumers of practical sensor nodes (i.e. sensors, transceivers, and CPU). Therefore, they cannot be directly applied for in-network processing optimization. More importantly, all current approaches are theoretical work without practical implementation. In contrast, our RWE has been implemented in Contiki OS and validate its practical performance in FIT IoT-LAB testbed.

2) In-network Processing.: A large number of approaches have been proposed for joint networking and in-network data processing, such as in-network fusion in traditional battery-based WSNs [9], [22]–[24], and in-network aggregation in data center networks [25]. However, to our knowledge there is no work existing on combining the in-network processing approach for EH-WSNs. Furthermore, the current schemes typically assume specific and constant network topologies (e.g. fixed trees). In contrast, our RWE can work in networks with general and time-varying topologies while adapting to, and fully exploiting, the time-varying harvested energy.

C. Paper Organization

The next section presents the system model. The RWE algorithm is proposed in Section III. Section IV provides discussions and the theoretical analysis of the RWE algorithm. We discussed the practical issues and implementation details of RWE in Section V. Testbed experiments and extensive trace-driven simulations are discussed in Section VI, and we conclude this paper in Section VII. The proofs of all theorems can be found in appendices (http://bit.ly/1MQQ1lo).

II. System Model

We consider an energy harvesting network that consists of a set of statically-deployed nodes $\mathcal{N} = \mathcal{S} \cup \mathcal{D}$, where $\mathcal{S}$ and $\mathcal{D}$ represent the sets of all sensor nodes and IoT gateways (sinks) respectively. The network can be modeled as a graph $G(\mathcal{N}, \mathcal{L})$ with arbitrary topologies, where $\mathcal{L}$ represents the set of all wireless links. Let $\mathcal{N}_x \subseteq \mathcal{N}$ be the set of all one-hop neighbors of each node $x \in \mathcal{N}$. The network operates in a finite-horizon period consisting of discrete time slots $t \in \{1,\ 2, ...,\ \mathrm{t_{end}}\},\ \mathrm{t_{end}} < \infty$. At each slot, a sensor node can have the following four operations: collecting raw sensor readings, performing processing on data packets in its data queue, transmitting or receiving data packets over wireless links.

A. Sensing and Communication Models

1) Sensing Model: At each slot t, every node x collects *raw data readings* from *hardware sensor* at a rate of $r_x(t) \geq 0$. We denote the per packet energy cost for the sensing operation (i.e. sensing price) of $x \in \mathcal{S}$ as $p^s_x(t)$, i.e. x's total energy cost for sensing is $r_x(t)p^s_x(t)$. In practice, $p^s_x(t)$ may be very different across nodes, depending on which type of sensor used by x. For instance, the sensing price of a camera is normally much higher than that of a temperature sensor.

2) Stochastic Link Capacity and Transmission Cost: Let $c_{x,y}(t) \geq 0$ be the time-varying capacity of wireless link $(x, y) \in \mathcal{L}$ at slot t, i.e. the maximum (integer) number of data packets that can be successfully transmitted from x to y during slot t, and $f_{x,y}(t) \leq c_{x,y}(t)$ be the actual number of data packets transmitted over wireless link (x, y) at slot t. In addition, denote $\mathrm{c_{max}} < +\infty$ as the finite upper bound of all channel capacities (e.g. $\forall t, \forall (x, y), c_{x,y}(t) \leq \mathrm{c_{max}}$), depending on the actual wireless radios of the sensor nodes.

Denote $p^t_{x,y}(t)$ and $p^r_{x,y}(t)$ as energy prices for the transmitter x and receiver y at time slot t respectively, for a successful transmission over wireless link (x, y) at slot t, i.e. total energy costs for transmitting and receiving at slot t are $f_{x,y}(t)p^t_{x,y}(t)$ and $f_{x,y}(r)p^r_{x,y}(t)$ respectively. It can be seen that both $p^t_{x,y}(t)$ and $p^r_{x,y}(t)$ depends on the power consumption of nodes' wireless transceivers and the channel quality of wireless link (x, y) at slot t (e.g. link-layer retransmissions).

3) Wireless Interference Model: Let the $|\mathcal{L}|$-dimensional vectors $\boldsymbol{c}(t)$ and $\boldsymbol{f}(t)$ represent link capacities and data transmission rates overs all wireless links in $\mathcal{L}$ at slot t, respectively. A set of wireless links are contention-free if all links in this set can be active (i.e. transmitting data) simultaneously, depending

on the interference relations among them. For a given $\boldsymbol{c}(t)$, we define a $|\mathcal{L}|$-dimensional contention-free link rate vector $\boldsymbol{\mu}(\boldsymbol{c}(t))$. Here, the l^{th} entry of $\boldsymbol{\mu}(\boldsymbol{c}(t))$ is the capacity c_l of the link l, if l is scheduled to transmit; otherwise, entry l is zero. The wireless links associated with the non-zero entries in $\boldsymbol{\mu}(\boldsymbol{c}(t))$ are contention free. We further define the link rate region $\Gamma(\boldsymbol{c}(t))$ as the set of all possible contention-free link rate vectors $\boldsymbol{\mu}(\boldsymbol{c}(t))$. At any slot t, a data transmission decision $\boldsymbol{f}(t)$ should satisfy the following constraint:

$$\boldsymbol{f}(t) \in \Gamma(\boldsymbol{c}(t)) \tag{1}$$

which captures both the physical and link layer constraints of wireless transmissions.

B. In-Network Data Processing Model

1) Data Buffer Model: Each sensor node $x \in \mathcal{S}$ maintains a data queue $\mathcal{Q}_x(t)$ to store its own sensed raw data packets, data packets processed by itself, and (raw and processed) data packets received from its neighbors in $\mathcal{N}_x$. Therefore, the queue $\mathcal{Q}_x(t)$ represents the set of data packets in node x's data queue at slot t.

Let $Q_x(t) \geq 0$ be the length of queue $\mathcal{Q}_x(t)$, i.e. $Q_x(t) = |\mathcal{Q}_x(t)|$. Since sensor nodes normally have limited RAM resources, we consider a *finite buffer size* $\mathrm{Q}_{\max}$ in our model, i.e. $\forall x, \forall t, Q_x(t) \leq \mathrm{Q}_{\max}$.

2) Data Processing Decisions: Assume each data packet m in the network has a unique type $\theta_m \in \Theta$ that identifies the properties of m, including its source ID, data attributes, correlation groups, Quality of Information (QoI), etc. Here, the type space Θ is a finite and countable set that includes all possible data types in a given network, which depends on specific network objectives. A data processing decision [7], [9], [26] of node x at slot t can be defined in a general form:

$$\xi_x^t : \times_{Q_x(t)}\Theta \rightarrow \times_{|\mathcal{Q}_x^{\xi}(t)|}\Theta \tag{2}$$

where $\mathcal{Q}_x^{\xi}(t) = \xi_x^t(\mathcal{Q}_x(t))$ represents the resulting set of processed data packets. It is worth noting that a reasonable local data processing decision ξ_x^t should not result in an increased queue length, i.e. $|\xi_x^t(\mathcal{Q}_x(t)| \leq Q_x(t)$. Data processing operations that increase data volume should be performed at the gateway, rather than inside the network.

It can be seen that each node x may be able to make various data processing decisions ξ_x^t, for a given $\mathcal{Q}_x(t)$. For instance, suppose $\mathcal{Q}_x(t)$ contains three data packets with readings $\{a, b, c\}$ and the processing objective is to aggregate the results and compute the average, then x has four choices of processing decisions: computing $(a+b)/2, (a+c)/2, (b+c)/2$, and $(a+b+c)/3$. Therefore, we can define the set of all possible processing decisions as Ξ_x^t.

Definition 1 [Shadow Sinks and Virtual Data forwarding]. *Define a shadow sink x' associated to each sensor node x with a virtual queue length $Q_{x'}(t) = 0,\ \forall t \geq 1$. A data processing decision ξ_x^t can be viewed as if x sends $\widetilde{f}_{x,x'}$ number of virtual data packets to its associated shadow sink x', where*

$$\widetilde{f}_{x,x'}(t) = Q_x(t) - |\xi_x^t(\mathcal{Q}_x(t))| \geq 0 \tag{3}$$

The capacity of shadow link (x, x') is defined as,

$$\widetilde{c}_{x,x'}(t) = \max_{\xi_x^t \in \Xi_x^t} (Q_x(t) - |\xi_x^t(\mathcal{Q}_x(t))|) \tag{4}$$

It can be seen that virtual data forwarding $\widetilde{f}_{x,x'}(t) \leq \widetilde{c}_{x,x'}(t)$ is similar to data forwarding over real-world wireless links.

3) Energy Cost of Local Data Processing: Since data processing operations are CPU-intensive, the energy consumption of a data processing $EC_x^{dp}(t)$ for node x at slot t depends on the computational complexity of corresponding processing rule ξ_x^t and the original data set before fusion $\mathcal{Q}_x(t)$. From (3), we can see that the virtual forwarding rate $\widetilde{f}_{x,x'}(t)$ is also a function of ξ_x^t and $\mathcal{Q}_x(t)$. We can write $EC_x^{dp}(t)$ as a function of $\widetilde{f}_{x,x'}(t)$, i.e. $EC_x^{dp}(\widetilde{f}_{x,x'}(t))$.

Here, $EC_x^{dp}(\widetilde{f}_{x,x'}(t))$ can be either a linear or a non-linear function of the virtual forwarding rate $\widetilde{f}_{x,x'}(t)$. Simple processing operations such as aggregations that are required to compute the maximal, minimal, and average data values normally result in a linear function. For instance, let e^1 and e^2 be the energy costs of atomic addition and division operations respectively. The energy consumption for average value computation can be easily obtained:

$$EC_x^{dp}(\widetilde{f}_{x,x'}(t)) = e^1\widetilde{f}_{x,x'}(t) + e^2$$

The function $EC_x^{dp}(\widetilde{f}_{x,x'}(t))$ could be non-linear, for more complex processing operations; such as Kalman-filter based data fusion, and image fusion [27], [28]. Due to the page limits, we do not discuss the detailed analysis for energy consumption of these processing operations in this paper.

C. Data Queue Length Dynamics

Consider the sensing, transmitting, receiving and data processing operations, it can be seen the queue length dynamics of a sensor node $x \in \mathcal{S}$ can be described as

$$Q_x(t) \leq \mathrm{Q}_{\max} \tag{5}$$

$$Q_x(t+1) = |Q_x(t) - f_x^{out}(t) - \widetilde{f}_{x,x'}(t)|_+ + r_x(t) + f_x^{in}(t) \tag{6}$$

where the operator $|a|_+$ means $\max(a, 0)$; and $f_x^{out}(t) = \sum_{y\in\mathcal{N}_x} f_{x,y}(t)$ and $f_x^{in}(t) = \sum_{y\in\mathcal{N}_x} f_{y,x}(t)$ represent the total numbers of transmitted and received packets at slot t respectively. The queue length of all sinks are always zero.

D. Models for Energy Harvesting, Storage, and Consumption

There are three key components in the embedded energy harvesting system of each sensor node: energy harvester, energy storage, and energy consumers. Specifically, consider a node $x \in \mathcal{S}$ at slot t, let $h_x(t) \geq 0$, $B_x(t) \geq 0$, and $EC_x(t) \geq 0$ be the amount of its harvested energy, residual battery level, and energy consumption respectively. In our model, we consider a battery with finite-capacity, i.e. $\forall x, t,\ B_x(t) \leq \mathrm{B}_{\max}$.

For a sensor node x at slot t, its total energy consumption $EC_x(t)$ is the sum of energy costs by operations for *sensing*, *transmitting*, *receiving*, and *data processing*

$$EC_x(t) = p_x^s(t) r_x(t) + EC_x^{dp}(t) + \sum_{y \in \mathcal{N}(t)} p_{x,y}^t(t) f_{x,y}(t) + \sum_{y \in \mathcal{N}(t)} p_{y,x}^r(t) f_{y,x}(t) \quad (7)$$

Considering the hardware of real sensor nodes, the total per-slot energy consumption $EC_x(t)$ should be upper bounded by a finite value $\mathrm{E_{max}}$ (i.e. $\forall x, t,\ E_x(t) \le \mathrm{E_{max}}$), which depends on the maximum total power consumption of sensor nodes and the duration of a slot. Generally, $\mathrm{E_{max}} \ll \mathrm{B_{max}}$, because $\mathrm{E_{max}}$ (typically in mJ) is multiple orders of magnitude smaller than $\mathrm{B_{max}}$ (typically in kJ) in practice.

The dynamic energy system of each can be modeled as:

$$0 < B_x(t) \le \mathrm{B_{max}},\ \forall x \in \mathcal{S}, 1 \le t \le \mathrm{t_{end}} \quad (8)$$

$$B_x(t+1) = B_x(t) - EC_x(t) + h_x(t),\ \forall x, t \quad (9)$$

Here, (9) represents the recharging and discharging process of the battery ; and (8) highlights the bounded battery capacity. More importantly, the constraint $\forall x, t,\ B_x(t) > 0$ ensures *sustainable operation*, which is expected to be achieved by every sensor node in the network, i.e. no node runs out of energy at any slot.

E. Optimization Objective

We *do not* make any probabilistic (e.g. specific distribution) and stochastic (e.g. Markov process) assumptions of the dynamic network states, including harvested energy, energy costs (for sensing, processing, transmitting, and receiving), as well as transmission and data processing capacities. The objective of this paper is to seek an algorithm that can solve the following finite-horizon stochastic optimization problem, by making sensing rate control $\boldsymbol{r}(t) = (r_1(t), ..., r_{|\mathcal{S}|}(t))$, wireless transmission $\boldsymbol{f}(t)$, and data processing $\widetilde{\boldsymbol{f}}(t)$ decisions at each slot $1 \le t \le \mathrm{t_{end}}$.

$$\underset{\boldsymbol{r}(t),\, \boldsymbol{f}(t),\, \widetilde{\boldsymbol{f}}(t)}{\textbf{maximize}} \quad \frac{1}{\mathrm{t_{end}}} \sum_{t=1}^{\mathrm{t_{end}}} \sum_{x \in \mathcal{S}} U_x(r_x(t)) \quad (10)$$

subject to

$$\boldsymbol{f}(t) \in \Gamma(\boldsymbol{c}(t)),\ 1 \le t \le \mathrm{t_{end}} \quad (11)$$

$$0 \le r_x(t) \le \mathrm{r_{max}},\ 1 \le t \le \mathrm{t_{end}}\ \forall x \in \mathcal{S} \quad (12)$$

$$0 \le \widetilde{f}_{x,x'}(t) \le \widetilde{c}_{x,x'}(t),\ 1 \le t \le \mathrm{t_{end}},\ \forall x \in \mathcal{S} \quad (13)$$

$$\frac{1}{\mathrm{t_{end}}} \sum_{t=1}^{\mathrm{t_{end}}} (EC_x(t) - h_x(t)) \le 0,\ \forall x \in \mathcal{S} \quad (14)$$

$$\frac{1}{\mathrm{t_{end}}} \sum_{t=1}^{\mathrm{t_{end}}} (f_x^{in}(t) + r_x(t) - f_x^{out}(t) - \widetilde{f}_{x,x'}(t)) \le 0 \quad (15)$$

Constraints (5), (6), (7), (8), and (9)

where the utility function $U_x(r_x(t)),\ x \in \mathcal{S}$ is a concave, differentiable and increasing function of sensing rate $r_x(t)$, such as the α-fairness utility function [29] that considers both throughput and fairness between sensing rates. The objective (10) is to maximize the time-average total sensor utilities over the time horizon of the system. Constraint (12) represents that the sample rate $r_x(t)$ is bounded by a finite value $\mathrm{r_{max}} < \infty$ in practice. Constraint (14) ensures that each node cannot consume more energy than it can harvest. Constraint (15) states that the total amount of each node's incoming data must be no more than that of its outgoing data.

III. RWE Algorithm

This section presents our RWE algorithm, a theoretically optimal solution to the stochastic problem formulated in Subsection II-E. At each slot t, RWE operates as follows:

1. **Sensing Rate Control.** Each node $x \in \mathcal{S}$, set its optimal sensing rate as

$$r_x^*(t) = \min(\mathrm{r_{max}}, U'^{-1}(\frac{Q_x(t) + p_x^s(t)(\mathrm{B_{max}} - B_x(t))}{V})) \quad (16)$$

where $V \ge 0$ is a system parameter which will be explained later. $U'^{-1}()$ represent the inverse function of the first derivative of utility $U()$. For instance, consider an approximate proportional fair utility $U(r_x(t)) = \ln(r_x(t) + 1)$, then $r_x^*(t) = \min(\mathrm{r_{max}}, V/(Q_x(t) + p_x^s(t)(\mathrm{B_{max}} - B_x(t))) - 1)$.

2. **Local Data Processing.** Each node $x \in \mathcal{S}$, compute its optimal processing action

$$\widetilde{f}_{x,x'}(t) = \begin{cases} \underset{0 \le \widetilde{f}_{x,x'}(t) \le \widetilde{c}_{x,x'}(t)}{\arg\max} \ g(\widetilde{f}_{x,x'}(t)) & \text{if } B_x(t) \ge \mathrm{E_{max}} \\ 0 & \text{otherwise} \end{cases} \quad (17)$$

where

$$g(\widetilde{f}_{x,x'}(t)) = Q_x(t)\widetilde{f}_{x,x'}(t) - EC_x^{dp}(\widetilde{f}_{x,x'}(t))(\mathrm{B_{max}} - B_x(t)) \quad (18)$$

For instance, consider a linear function $EC_x^{dp}(\widetilde{f}_{x,x'}(t)) = p_x^{dp}(t)\widetilde{f}_{x,x'}(t)$. Objective (18) can be easily maximized by setting $\widetilde{f}_{x,x'}(t) = \widetilde{c}_{x,x'}(t)$, if $Q_x(t) - p_x^{dp}(t)(\mathrm{B_{max}} - B_x(t)) > 0$. Otherwise, $\widetilde{f}_{x,x'}(t)$ can be set as zero to maximize (18).

3. **Scheduling.** For each link $(x, y) \in \mathcal{L}$, compute a weight

$$w_{x,y}(t) = \begin{cases} \hat{w}_{x,y}(t) & \text{if } (\frac{Q_y(t)}{\mathrm{Q_{max}} - \eta} < 1) \wedge (B_x(t), B_y(t) \ge \mathrm{E_{max}}) \\ 0 & \text{otherwise} \end{cases} \quad (19)$$

where $\eta = \mathrm{r_{max}} + \mathrm{c_{max}}$ and

$$\hat{w}_{x,y}(t) = Q_x(t) - Q_y(t) - p_{x,y}^t(t)(\mathrm{B_{max}} - B_x(t)) - p_{x,y}^r(t)(\mathrm{B_{max}} - B_y(t)) \quad (20)$$

Then compute the contention-free link with maximum aggregated weights,

$$\mu^*(t) = \arg \max_{\mu(t) \in \mathbb{L}^f} \sum_{(x,y) \in \mu(t)} w_{x,y}(t) \quad (21)$$

Where $\mathbb{L}^f \subset 2^{\mathcal{L}}$ is the set of all contention-free links. For general interference relations, the optimal solution to the scheduling problem (21) is centralized and NP-hard (e.g. [30]), which is therefore intractable in practice. Therefore,

we implemented a fully distributed suboptimal scheduler, the lightweight *Longest Queue First (LQF)*, which have the potential to achieve a near-optimal performance in practice [31]–[33]. *Here, RWE with optimal and distributed LQF schedulers are named as REW-opt and RWE-dist respectively.*

4. **Data Forwarding.** The data forwarding rate $f_{x,y}(t)$ over each link $(x,y) \in \mathcal{L}$ is set according to

$$f_{x,y}(t) = \begin{cases} c_{x,y}(t) & \text{if } w_{x,y} > 0 \text{ and } (x,y)^u \in \mathcal{M}(t) \\ 0 & \text{otherwise} \end{cases} \quad (22)$$

5. **Data and Energy Queue Update.** After performing the sensing, data processing, and data forwarding operations, each sensor node x updates its battery level using (9) and (8), and queue backlog according to (5) and (6).

IV. Analytical Results

This section presents the discussions and theoretical analysis of the RWE performance.

A. Discussions

By using RWE, each sensor node makes the optimal decisions in real-time and in a fully distributed manner (i.e. RWE-dist, when adopts distributed matching). These decisions are based on the *current* system states only, and no knowledge regarding the future network state is required by RWE.

1) Control Overheads and Scalability: The RWE-dist has three types of control overheads

- **Communication Overhead.** At each slot, every node broadcasts a beacon to communicate its queue backlog to its one-hop neighbors. For distributed scheduling, each node transmits at most one control packet to each of its neighbors [31], [34], [35]. Hence, the communication overhead of RWE-dist is $O(D)$ per node per slot, where D is the average node degree of the EH-WSN.
- **Computational Overhead.** At each slot t, every node $x \in \mathcal{S}$ performs two simple arithmetic calculations for sensing and data processing, and $|\mathcal{N}_x|$ simple arithmetic calculations for scheduling and data forwarding. Consequently, the computational overhead of RWE-dist is $O(D)$ per node per slot.
- **Storage Overhead.** The simple operations required by RWE result in relatively easy implementation (also small size of programming code) and therefore small usage of ROM. Furthermore, the RAM occupation is also limited, Since the sizes of all data queues are deterministically bounded by $\mathrm{Q_{max}}$.

In summary, the RWE-dist algorithm is *scalable*, since the per-node overheads of RWE for communication, computation, and storage are independent to the network size $|\mathcal{N}|$.

B. Analytical Results

1) Asymptotically Optimality: We divide the time horizon of the system, $1 \le t \le \mathrm{t_{end}}$, into K successive frames with size of T slots (i.e. $\mathrm{t_{end}} = KT$). Assuming that there exists an *ideal* algorithm operating in the first slot of each frame $k = KT - T + 1, 1 \le K \le \mathrm{t_{end}}/T$ that can obtain full information during the future T slots (i.e. the future energy budget and parameters, channel qualities, and data processing opportunities of all nodes in the kth frame). Based on future knowledge, the ideal algorithm solves the following optimization problem:

$$\underset{\boldsymbol{r}(t),\, \boldsymbol{f}(t),\, \widetilde{\boldsymbol{f}}(t)}{\textbf{maximize}} \quad \frac{1}{T} \sum_{t=kT}^{kT-T+1} \sum_{x \in \mathcal{S}} U_x(r_x(t)) \quad (23)$$

s.t.

$$\sum_{t=kT-T+1}^{kT} (\widetilde{f}_{x,x'}(t) + f_x^{out}(t) - f_x^{in}(t) - r_x(t)) \ge 0 \quad (24)$$

$$\sum_{t=kT-T+1}^{kT} (EC_x(t) - h_x(t)) \le 0, \ \forall x \in \mathcal{S} \quad (25)$$

$$\text{per-slot constraints}: \ (5)\text{-}(9), \text{ and } (11)\text{-}(13)$$

The objective (23) demonstrates that the ideal algorithm optimizes the global social utility over each frame $1 \le k \le K$. Define the $U_k^{ideal}(T)$ to be the optimal aggregated utility (23) achieved by the ideal algorithm for the kth T-slot frame. Due to the complete future knowledge requirement, it is impossible to design such an ideal algorithm to achieve $U_k^{ideal}(T)$ in practice. However, $U_k^{ideal}(T)$ can be used as a performance baseline.

Theorem 1. *Part 1: If the optimal (centralized) scheduler is adopted, the time-average aggregate utility achieved by RWE-opt satisfies:*

$$\overline{U}_{opt} = \frac{1}{KT} \sum_{t=1}^{KT} U(t) \ge \frac{1}{K} \sum_{k=1}^{K} U_k^{ideal}(T) - \frac{MT + Z}{V} \quad (26)$$

where

$$M = \frac{1}{2}|\mathcal{S}|((\mathrm{c_{max}} + \max(\mathrm{r_{max}}, \widetilde{\mathrm{c}}_{\max}))^2 + \max(\mathrm{h_{max}^2}, \mathrm{E_{max}^2}))$$

$$\begin{aligned} Z \ = \ & |\mathcal{S}| \max(\mathrm{E_{max}}, \mathrm{h_{max}}) \mathrm{B_{max}} \\ & + |\mathcal{S}|^2 (\mathrm{c_{max}^2} + \mathrm{c_{max}} \max(\mathrm{r_{max}}, \widetilde{\mathrm{c}}_{\max})) \end{aligned}$$

are constant values

Part 2: Under the node-exclusive interference model (e.g. [31]), the time-average aggregate utility achieved by RWE-dist with distributed greedy scheduler satisfies:

$$\overline{U}_{dist} \ge \frac{1}{2K} \sum_{k=1}^{K} U_k^{ideal}(T) - \frac{MT + Z}{V} \quad (27)$$

Proof. The proof of Theorem 1 can be found in Appendix A (http://bit.ly/1MQQ1lo). □

When $T = \mathrm{t_{end}}$, the ideal algorithm is the optimal solution to the problem (10), therefore $\overline{U}_{opt} \le U_k^{ideal}(\mathrm{t_{end}})$. In addition, as $(M\mathrm{t_{end}} + Z)/V$ are a constant value, RWE-opt asymptotically achieves the optimal, as $V \to +\infty$.

2) Deterministic Bounded Data Queue: Memory is a limited resource for typical low-cost sensor nodes. Theorem 2 below shows that all data queue backlogs are deterministically bounded by using RWE.

Theorem 2. *Suppose the initial queue backlogs is empty, i.e.* $Q_x(1) = 0,\ \forall x \in \mathcal{S}$, *then* $Q_x(t)$ *is always less than* $\mathrm{Q}_{\max},\ \forall t \geq 1$, *if*

$$V \leq \min_{x\in\mathcal{S}}(\mathrm{Q}_{\max} - \eta)/U'_x(0) \tag{28}$$

Proof. The proof of Theorem 2 can be found in Appendix B (http://bit.ly/1MQQ1lo). □

In practice, $\eta, U'_x(0)$, and $\mathrm{Q}_{\max}$ are normally fixed and can be determined in advance. Therefore, the parameter V can be set to guarantee the inequality (28). For instance, if the utility function of a sensing x is chosen as $U_x(r_x(t)) = \ln(r_x(t)+1)$, then $U'_x(0) = 1$ and V can be smaller than $\mathrm{Q}_{\max} - \eta$ to avoid packet drops caused by data buffer overflow.

3) Sustainable Network Operation.: A key objective of our design is to achieve sustainable network operation. Theorem 3 below demonstrates the RWE can achieve the strong guarantee of sustainable network operation.

Theorem 3. *Sustainable network operation can be guaranteed by RWE, if* $B_x(1) > 0, \forall x \in \mathcal{S}$ *and*

$$V \leq \min_{x\in\mathcal{S}} \mathrm{E}_{\max}(\mathrm{B}_{\max} - \mathrm{E}_{\max})/U'_x(0) \tag{29}$$

Proof. The proof of Theorem 3 can be found in Appendix C (http://bit.ly/1MQQ1lo) □.

V. Implementation of RWE-dist

We implemented RWE-dist in Contiki [13], an open source operating system for WSNs and the Internet of Things (IoTs). This section highlights key details of our implementation.

A. RWE in CSMA-based EH-WSNs

RWE uses slotted Time Division Multiple Access (TDMA), yet most current commercial short-range wireless radios are based on Carrier Sense Multiple Access (CSMA), such as the IEEE 802.15.4 radio used in our evaluation. To implement the TDMA-based RWE over a CSMA network, we used a simple technique proposed in [36]: If a wireless link is scheduled to transmit, the corresponding transmitter will reduce the size of its CSMA back-off window to aggressively access the channel; otherwise, it will access the channel with normal back-off window size.

B. An Example Data Processing Rule: Correlation-Group Based in-network Fusion/Aggregation

It can be seen that RWE can be used for any in-network data processing applications, as long as the processing rule for each sensor node x can be determined. To evaluate the practical performance of RWE, we implemented a simple but typical data processing rule, which is described as follows:

- All sensor nodes with unique positive IDs are divided into multiple groups with same sensor types and unique group IDs. Each raw or fused packet has a format as shown in Fig.1. When a raw data packet is produced by a sensor node x in group g, the header segments of this packet are set as SOURCE ID= x, GROUP ID= g.
- A set of raw data packets with the same GROUP ID and different SOURCE ID values can be fused, which will result in a fused data packet with the same GROUP ID and a SOURCE ID with a value of -1.
- A set of hybrid fused and raw data packets with the same group ID can be further fused. The SOURCE ID of the new fused packet is assigned -1.

Fig. 1. Data packet format in our implementation.

It can be seen that above correlation-group based in-network fusion/aggretation captures realistic characteristics of a large class of applications. For instance, above rule can represent the in-network aggregation computations of the average, maximal, and minimal of spatial-correlated sensor readings (e.g. temperature, air condition, and noise). In addition, this fusion rule can also be pixel-level multi-sensor image fusion such as [27], [37], which combines multiple images produced by different types sensors into a single image. For brevity, our implementation assumes the energy consumption of data processing $EC_x^{dp}(\widetilde{f}_{x,x'}(t))$ takes a simple linear form

$$EC_x^{dp}(\widetilde{f}_{x,x'}(t)) = p_x^{dp} f_{x,x'}(t), \forall x \in \mathcal{S} \tag{30}$$

where the per packet processing price p_x^{dp} depends on the computational complexity of the specific data processing operation. Table I below summarizes our implementation details.

TABLE I
Implementation details

Operating System	Testbed	ROM	RAM	MAC
Contiki	FIT IoT-LAB	6 kB	3.5 kB	CSMA+LQF

VI. Evaluation

We performed our evaluation experiments for RWE-dist on 100 sensor nodes (M3 Open Nodes) selected from the Lille site offered by FIT IoT-LAB testbed [14], as shown in Fig. 2 (a) and (b).

Each M3 open node has a ARM Cortex M3 microcontroller, a 64 kB RAM, a IEEE 802.15.4 radio AT86RF231, several types of sensors, and a rechargeable 3.7 V LiPo battery ($\mathrm{B}_{\max} = 650$ mAh, around 8.7 Kilojoules). The transmission power was set as -17 dBm.

We used a one-month real solar data trace [38] shown in Fig.2 (c)[1] as the energy source in our evaluations. In our

[1]Since the solar data granularity is five minutes, each slot (i.e. a second) in our evaluation represents 300 seconds in reality. This significantly increased the evaluation speed, and enabled us to evaluate the one-month performance of RWE-dist within 2.5 hours.

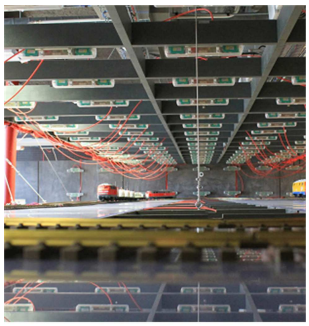

(a) sensor node deployment

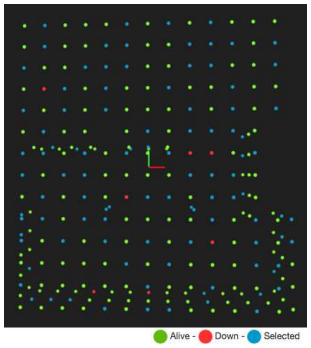

(b) network topology

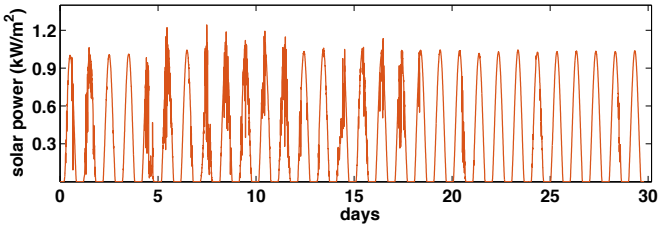

(c) real solar data

Fig. 2. Experiment Settings:(a) Node deployment in FIT IoT-LAB; (b) The network topology of the EH-WSN in the FIT IoT-LAB experiments, the blue node at the right-bottom corner is the sink while other blue nodes are sensor nodes; and (c) One-month real solar power data used in our evaluation [38].

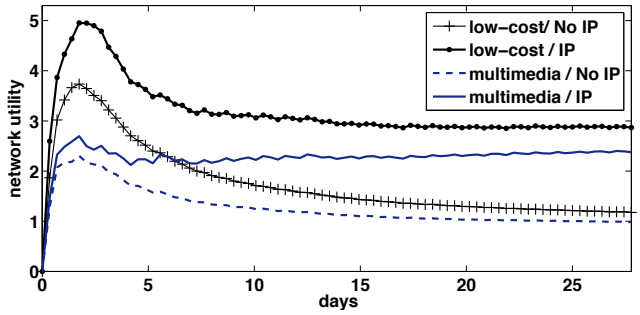

(a) Time-average Network Utility

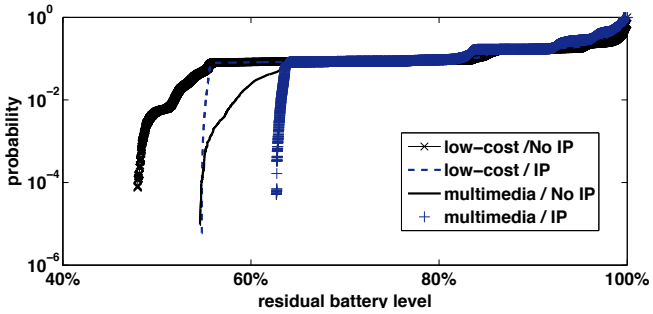

(b) CDF of Battery Levels

Fig. 3. Testbed experiment results: the network utility and sustainable operation performance of RWE for low-cost and multimedia sensing applications.

evaluation, the duration of a slot was set as one second. We consider typical solar powered sensor nodes, each of which is equipped with a $3.8\text{cm} \times 9\text{cm}$ solar panel (with a photovoltaic transfer efficiency of 50% [39]). In order to model the heterogeneous solar harvesting opportunities over the networks, we added random noise equating to $\pm 50\%$ to the original solar data for each sensor node.

According to the datesheet of the AT86RF231 (i.e. the IEEE 802.15.4 transceiver used in our selected M3 sensor nodes), the current consumption for data receiving and transmitting (at -17dBm) are 12.3 mA and 7.4 mA respectively. Therefore, we should set $p^t_{x,y}(t) = 0.6p^r_{x,y}(t)$ for each wireless link (x, y) at every slot t. Furthermore, considering the dynamic channel quality of the IEEE 802.15.4 wireless channels, we set the time-varying per-packet receiving price $p^r_{x,y}(t) = 5ETX_{x,y}(t)$ and transmitting price $p^t_{x,y}(t) = 0.6p^r_{x,y}(t) = 3ETX_{x,y}(t)$ (in mJ per packet). Here, $ETX_{x,y}(t)$ is the ETX value of over wireless link (x, y) at slot t, which was measured at real-time.

For the sensing and data processing energy pricing, we considered two sets of typical applications: *low-cost sensing* and *multimedia sensing*, which represent simple (e.g. temperature samples) and complex (e.g. image) sensor data structures respectively. For the low-cost sensing, the time-varying sensing price $p^s_x(t)$ and data processing price $p^{dp}_x(t)$ were randomly assigned using a uniform distribution over a range of [1, 2] (mJ per packet) for each sensor node x and slot t; For the multimedia sensing, the ranges of sensing and data processing price are [6, 8] mJ per packet. In addition, other

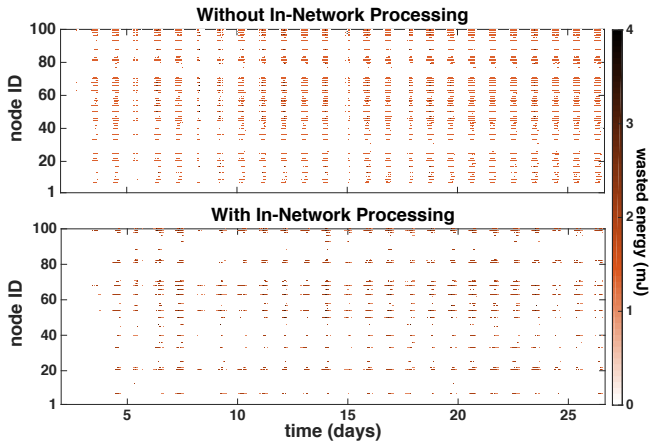

(a) wasted energy visualization (low-cost sensing)

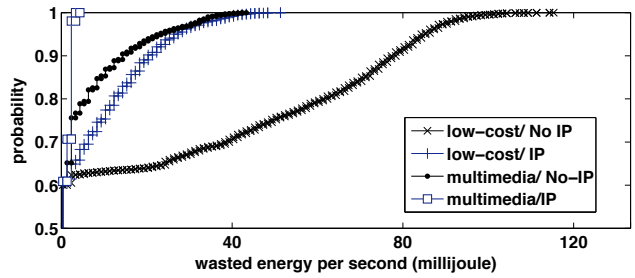

(b) CDF of Wasted Energy Per Second

Fig. 4. Testbed experiment results: the impact of in-network data processing (IP) on energy utilization.

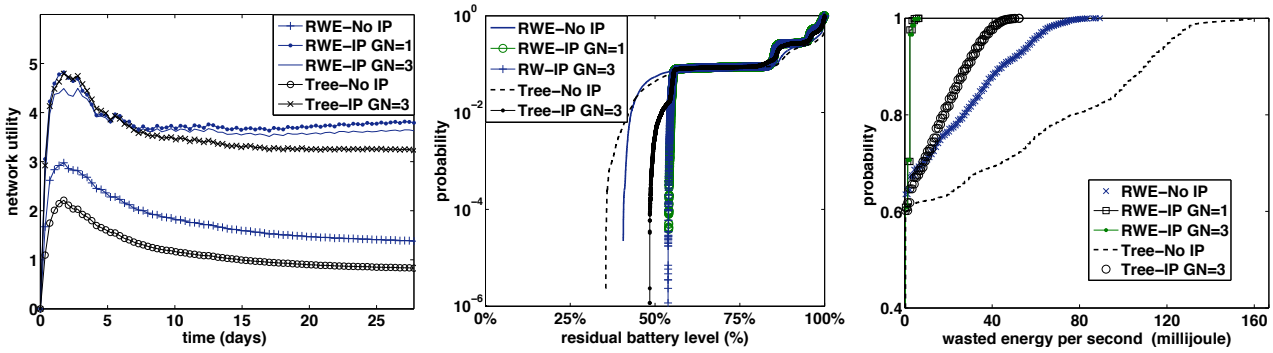

(a) Time-average Network Utility (b) CDF of Battery Level (c) CDF of Wasted Energy

Fig. 5. Simulation results on Cooja: the impacts of data processing capacity and underlying routing topology on the network performance.

parameters were set as $U_x(r_x(t)) = \ln(1+r_x(t))$, $\mathrm{r_{max}} = 10$, $\eta = 50$, and $V = 150$, $\mathrm{Q_{max}} = 200$.

A. Testbed Experiments

1) Network Utility and Battery Performance: Fig.3 shows the network utility and battery performance for that RWE with in-network data processing (IP) and without in-network processing (referred as No IP, i.e. joint optimization for sensing and networking only). The *network utility* in Fig.3(a) is the time-average value at each slot t is computed as $\sum_{\tau=1}^{t}\sum_{x\in S}\ln(1+r_x(\tau))/t$. It can been seen that around 200% and 150% utility improvements are achieved by adopting in-network processing for low-cost and multimedia experiments. The fluctuations that appear in the time-average network utility curves are caused by the periodically changing solar power, which also demonstrate the adaptability of RWE.

Fig.3(b) shows the Cumulative Distribution Function (CDF) for the battery levels collected at every second. Due to the intermittent availability of solar energy, battery should be charged during the day time in order to power network during each night. RWE combines the optimization of battery management and devices operations (sensing, transmitting, receiving, and data processing), which ensures the sustainable operations in all experiments.

2) Improve The Harvested Energy Utilization: Due to limited energy harvesting capacities for typically tiny-size sensor nodes, harvested energy is still an scare resource, which should be utilized as much as possible. Fig.4 (a) visualizes the amount wasted energy of the all devices in the network during the whole duration of the two low-cost sensing experiments. It can be seen that energy was wasted periodically, during the strong solar radiation time of each day (normally between 1:00 PM to 3:00 PM), caused by battery overflow. This result shows that in-network data processing manages to recycle a significant amount of wasted energy, which is used to further improve the network utility. Fig.4 (b) shows the CDF of the wasted energy for all four experiments. In addition, by recycling waste energy for in-network processing operations, RWE reduced wasted energy by more than 75% for both low-cost and multimedia sensing experiments.

B. Trace-driven Simulation based on Cooja

To further study the performance of RWE-dist, we also construct simulations with a 100-node randomly-deployed EH-WSN (99 sensor nodes and a sink) on Cooja, the simulator of Contiki OS [13]. In all simulations, we only consider *low-cost sensing* scenarios. All other parameters, including the network utility, are the same as the testbed experiment settings.

Fig.5 demonstrates the impact of data processing capacity and underlying routing topology on the network performance. Here, the data processing capacity (i.e. $\widetilde{c}_{x,x'}(t),\ x\in\mathcal{S},\ t\geq 1$) was changed, by controlling the number of correlation groups (GN=1 and GN=3 in Fig.5). As the number of correlation groups increases, the average group size decreases resulting in a smaller data processing capacity at each node, according to the data processing rule defined in Subsection V-B. Fig.5(a) and (c) clearly show that larger group number (i.e. GN=3) results in worse network utility and energy utilization, due to the smaller in-network processing opportunities and capacities.

We also test two underlying routing topologies for RWE: no predetermined routing structure (i.e. the original RWE) and a tree (i.e. RWE with a fixed single path route). It can be seen that RWE can work with any network topology or underlying routing structures, but nearly all current in-network processing (fusion) approach in WSNs are based on fixed trees. Fig.5(a) and (c) show that restricted routing topology (i.e. tree) leads to lower network utility and worse energy utilization for RWE with and without in-network processing. Interestingly, the performance gain of using in-network processing in routing tree simulations are higher than that with unrestricted routing structures. Specifically, in-network processing results in around 300% improvement of average network utility (3.25 with IP and 0.83 without IP) and 97% reduction of average wasted energy (0.73 with IP and 30.4 without). Finally, Fig.5(b) shows that all the 5 variants of RWE achieve sustainable network operation.

VII. Conclusion

In this paper, we studied how to jointly optimize networking and in-network data processing in energy harvesting WSNs (EH-WSNs). We develop a novel technique called

shadow sink to map data processing operations to virtual data forwarding over virtual links. This enables us to formulate a stochastic network problem for joint optimization of in-network data processing and networking (sensing rate control, routing, scheduling) for EH-WSNs with general topologies and data processing rules, which aims to maximize network utility while ensuring sustainable operations. To solve the formulated problem, we develop an adaptive algorithm, Recycling Wasted Energy (RWE), which makes the real-time sensing, wireless transmission and data processing decisions in a distributed and adaptive way. To our knowledge, RWE is not only the first work on in-network data processing in EH-WSNs, but also the first approach that applies in-network data processing to the Lyapunov optimization framework.

Through rigorous analysis, we formally prove that RWE manages to achieve asymptotical optimality, bounded data queue size, and sustainable network operation. We implement RWE on a popular IoT operating system Contiki OS, and evaluate its performance through both real-world experiments using the FIT IoT-LAB testbed and extensive trace-driven simulations using Cooja. The evaluation results demonstrate that RWE can achieve significant performance improvements, in terms of harvested energy utilization and global network utility. Interesting future work is to evaluated practical data processing functions such as aggregate queries and entropy-based image fusion.

REFERENCES

[1] S. Yang, X. Yang, J. A. McCann, T. Zhang, G. Liu, and Z. Liu, "Distributed networking in autonomic solar powered wireless sensor networks," *IEEE J. Sel. Areas Commun.*, vol. 31, no. 12, pp. 750–761, 2013.

[2] P. D. Mitcheson, E. M. Yeatman, G. K. Rao, A. S. Holmes, and T. C. Green, "Energy harvesting from human and machine motion for wireless electronic devices," *Proc. IEEE*, vol. 96, no. 9, pp. 1457–1486, 2008.

[3] A. Kurs, A. Karalis, R. Moffatt, J. D. Joannopoulos, P. Fisher, and M. Soljačić, "Wireless power transfer via strongly coupled magnetic resonances," *science*, vol. 317, no. 5834, pp. 83–86, 2007.

[4] L. Huang and M. J. Neely, "Utility optimal scheduling in energy-harvesting networks," *IEEE/ACM Trans. Netw..*, vol. 21, no. 4, pp. 1117–1130, 2013.

[5] C. Tapparello, O. Simeone, and M. Rossi, "Dynamic compression-transmission for energy-harvesting multihop networks with correlated sources," *IEEE/ACM Trans. Netw.*, 2013.

[6] M. Chen, S. Mao, and Y. Liu, "Big data: A survey," *Mobile Networks and Applications*, vol. 19, no. 2, pp. 171–209, 2014.

[7] E. F. Nakamura, A. A. Loureiro, and A. C. Frery, "Information fusion for wireless sensor networks: Methods, models, and classifications," *ACM Comput. Surv*, vol. 39, no. 3, p. 9, 2007.

[8] P.-Y. Chen, S. Yang, and J. McCann, "Distributed real-time anomaly detection in networked industrial sensing systems," *IEEE Trans. Ind. Electron..*, vol. 62, no. 6, pp. 3832–3842, 2015.

[9] E. Fasolo, M. Rossi, J. Widmer, and M. Zorzi, "In-network aggregation techniques for wireless sensor networks: a survey," *IEEE Wireless Commun.*, vol. 14, no. 2, pp. 70–87, 2007.

[10] L. J. van der Maaten, E. O. Postma, and H. J. van den Herik, "Dimensionality reduction: A comparative review," *Journal of Machine Learning Research*, vol. 10, no. 1-41, pp. 66–71, 2009.

[11] N. Tang, "Big data cleaning," in *Web Technologies and Applications*, 2014, pp. 13–24.

[12] M.Neely, "Stochastic network optimization with application to communication and queueing system," *Morgan & Claypool Publishers*, 2010.

[13] http://www.contiki.com//.

[14] https://www.iot-lab.info/.

[15] S. Sudevalayam and P. Kulkarni, "Energy harvesting sensor nodes: Survey and implications," *IEEE Commun. Surveys Tuts.,*, vol. 13, no. 3, pp. 443–461, 2011.

[16] Z. Liu, X. Yang, S. Yang, and J. McCann, "Efficiency-aware: Maximizing energy utilization for sensor nodes using photovoltaic-supercapacitor energy systems," *International Journal of Distributed Sensor Networks*, 2013.

[17] M. Gorlatova, A. Wallwater, and G. Zussman, "Networking low-power energy harvesting devices: Measurements and algorithms," *IEEE Trans. Mobi. Comput.*, vol. 12, no. 9, pp. 1853–1865, 2013.

[18] J. Yang, X. Wu, and J. Wu, "Optimal scheduling of collaborative sensing in energy harvesting sensor networks," *IEEE J. Sel. Areas Commun.*, vol. 33, no. 3, pp. 512–523, 2015.

[19] S. Yang and J. A. McCann, "Distributed optimal lexicographic max-min rate allocation in solar-powered wireless sensor networks," *ACM Transactions on Sensor Networks*, vol. 11, no. 1, p. 9, 2014.

[20] L. Xie, Y. Shi, Y. T. Hou, W. Lou, H. D. Sherali, and S. F. Midkiff, "Bundling mobile base station and wireless energy transfer: Modeling and optimization," in *Proc. IEEE INFOCOM*, 2013, pp. 1636–1644.

[21] S. Sarkar, M. Khouzani, and K. Kar, "Optimal routing and scheduling in multihop wireless renewable energy networks," *IEEE Trans. Autom. Control*, vol. 58, no. 7, pp. 1792–1798, 2013.

[22] A. Manjhi, S. Nath, and P. B. Gibbons, "Tributaries and deltas: Efficient and robust aggregation in sensor network streams," in *Proc. ACM SIGMOD*, 2005, pp. 287–298.

[23] H. Luo, Y. Liu, and S. K. Das, "Distributed algorithm for en route aggregation decision in wireless sensor networks," *IEEE Trans. Mobi. Comput.*, vol. 8, no. 1, pp. 1–13, 2009.

[24] H. Luo, H. Tao, H. Ma, and S. K. Das, "Data fusion with desired reliability in wireless sensor networks," *IEEE Trans. Parallel Distrib. Syst.*, vol. 22, no. 3, pp. 501–513, 2011.

[25] L. Mai, L. Rupprecht, A. Alim, P. Costa, M. Migliavacca, P. Pietzuch, and A. L. Wolf, "Netagg: Using middleboxes for application-specific on-path aggregation in data centres," in *Proc. ACM CoNEXT*, 2014, pp. 249–262.

[26] H. Luo, Y. Liu, and S. K. Das, "Routing correlated data in wireless sensor networks: A survey," *IEEE Netw.*, vol. 21, no. 6, pp. 40–47, 2007.

[27] L. J. Chipman, T. M. Orr, and L. N. Graham, "Wavelets and image fusion," in *SPIE's 1995 International Symposium on Optical Science, Engineering, and Instrumentation*, 1995, pp. 208–219.

[28] H. Luo, J. Luo, Y. Liu, and S. K. Das, "Adaptive data fusion for energy efficient routing in wireless sensor networks," *IEEE Trans. Comput.*, vol. 55, no. 10, pp. 1286–1299, 2006.

[29] J. Mo and J. Walrand, "Fair end-to-end window-based congestion control," *IEEE/ACM Trans. Netw.*, vol. 8, no. 5, pp. 556–567, 2000.

[30] G. Sharma, R. Mazumdar, and N. Shroff, "On the complexity of scheduling in wireless networks," in *Proc. ACM Mobicom*, 2006, pp. 227–238.

[31] L. Chen, S. Low, M. Chiang, and J. Doyle, "Cross-layer congestion control, routing and scheduling design in ad hoc wireless networks," in *Proc. IEEE Infocom*, 2006, pp. 1–13.

[32] C. Joo, X. Lin, and N. Shroff, "Understanding the capacity region of the greedy maximal scheduling algorithm in multihop wireless networks," *IEEE/ACM Trans. Network.*, vol. 17, no. 4, pp. 1132–1145, 2009.

[33] A. Brzezinski, G. Zussman, and E. Modiano, "Enabling distributed throughput maximization in wireless mesh networks: a partitioning approach," in *Proc. ACM Mobicom*, 2006, pp. 26–37.

[34] J.-H. Hoepman, "Simple distributed weighted matchings," *arXiv preprint cs/0410047*, 2004.

[35] S. Yang, Z. Sheng, J. McCann, K. K. Leung *et al.*, "Distributed stochastic cross-layer optimization for multi-hop wireless networks with cooperative communications," *IEEE Trans. Mobile Comput.*, vol. 13, no. 10, pp. 2269–2282, 2014.

[36] U. Akyol, M. Andrews, P. Gupta, J. Hobby, I. Saniee, and A. Stolyar, "Joint scheduling and congestion control in mobile ad-hoc networks," in *Proc. IEEE Infocom*, 2008, pp. 619–627.

[37] G. Piella, "A general framework for multiresolution image fusion: from pixels to regions," *Information fusion*, vol. 4, no. 4, pp. 259–280, 2003.

[38] http://solardat.uoregon.edu/SolarData.html.

[39] O. López-Lapeña, M. T. Penella, and M. Gasulla, "A new mppt method for low-power solar energy harvesting," *IEEE Trans. Ind. Electron.*, vol. 57, no. 9, pp. 3129–3138, 2010.